Can Tho University Journal of Science
website: sj.ctu.edu.vn

DOI: 10.22144/ctu.jen.2020.009

Docking belinostat into HDAC 8 using autodock tool

Huynh Nhu Thao, Nguyen Huu Toan, Nguyen Thanh Si, Nguyen Cuong Quoc, Ha Thi Kim Quy, Le Thi Bach, Nguyen Trong Tuan, Bui Thi Buu Hue and Tran Quang De*

Department of Chemistry, College of Natural Sciences, Can Tho University, Vietnam

**Correspondence: Tran Quang De (email: tqde@ctu.edu.vn)*

Article info.

Received 04 Mar 2020
Revised 23 Apr 2020
Accepted 31 Jul 2020

Keywords

Autodock4, Autodock4Zn, HDAC 8, metalloenzymes

ABSTRACT

Belinostat, a histone deacetylases inhibitor, was reached the marketing approval by FDA for the treatment of relapsed and refractory peripheral T-cell lymphomas in 2014. Among 18 Histone Deacetylase (HDAC) enzymes, HDAC 8 has grabbed considerable attention from chemists as a promising target for cancer treatment, which leads to an ever-growing demand for the discovery of novel HDAC 8 inhibitors. With the advent of technologies, a useful and free-of-charge software – Autodock Tool was introduced to dock belinostat into the active site of HDAC 8 in this report. Nevertheless, docking to HDACs, known as metalloenzymes, still remains a challenge due to the interaction with Zn^{2+} ion at the bottom of the active binding site of the enzyme. For this reason, the extension of the Autodock forcefield to the new one named Autodock4Zn was utilized. The outcomes showed significant improvements in performance in both free energy of binding estimation as well as binding capacity of belinostat with different amino acids of HDAC8.

Cited as: Thao, H.N., Toan, N.H., Si, N.T., Quoc, N.C., Quy, H.T.K., Bach, L.T., Tuan, N.T., Hue, B.T.B. and De, T.Q., 2020. Docking belinostat into HDAC 8 using autodock tool. Can Tho University Journal of Science. 12(2): 1-8.

1 INTRODUCTION

There are 18 HDAC enzymes reported in total (Haberland *et al*., 2009), which are classified into four different groups including class I (HDACs 1, 2, 3, and 8), class II (HDACs 4, 5, 6, 7, 9, and 10), class IV (HDAC 11) and class III (sirtuin family: sirt1-sirt7) (De Ruijter *et al*., 2003). Ideally, histone deacetylase enzymes are promising targets for the development of anticancer drugs (Walkinshaw, 2008). The acetylation homeostasis in a normal cell is balanced by the control of histone deacetylase (HDAC) and histone acetylase (HAT) (Saha and Pahan, 2006). Pertubation of this balance shifted more towards HDAC may result in uncontrolled cell proliferation, loss of differentiation, an inhibition of apoptosis, loss of adhesion, migration and angiogenesis (Parbin *et al.*, 2014). Whereas, HDAC 1-3 and 6 drew enormous attention in the past (Falkenberg & Johnstone, 2014), the isotype HDAC8 has become the center of discussion in recent years (Mottamal *et al*., 2015). This change is due to the recognition of the difference in the sequence alignment in comparison with other class I enzymes (Ortore *et al*., 2009). HDAC8 was the only enzyme which shows slight difference variation compared with the rest of the class members. Further studies on HDAC8 have found that it was the main cause of deregulation and overexpression of genes due to its interaction with transcription

factors (Chakrabarti *et al.*, 2015). HDAC8 is also correlated with childhood neuroblastoma T-cell lymphoma (Kelly *et al.*, 2005). It is possible that isoform selectivity can be developed from subtle differences in the HDAC active site amino acids. The first noticeable feature which can be used for the design of HDAC8 selective structure is the formation of the foot pocket. This pocket can only be seen in class I (1, 2, 3, 8) but not in class II isotypes (Chakrabarti *et al*., 2016). The difference in the structure brings about preferences to different ligands. While class I HDACs prefer compounds with large frames occupying the foot pocket, class II HDACs tend to fill its small cavity with compact groups. Another characteristic is the presence of the side pocket near the main pocket (Micelli and Rastelli, 2015). This is the reason why class I HDACs 1-3 show favor to rod-shaped ligands such as SAHA, whereas compounds with bulky linkers (phenylene spacers) in combination with ortho- or meta- substituted cinnamic acid linkers are better inhibitors of HDAC8 (Krennhrubec *et al*., 2007; Balasubramanian *et al*., 2008; Olson *et al*., 2013).

Recently, molecular modelling has become a valuable tool in drug design process as it could present information on how a drug interacts with its receptor. The structure-based design of potent HDAC8 selective inhibitors using molecular modelling protocols has been made possible by the availability of the 3D structure of HDAC8, which was elucidated in 2004. Based on the crystal structure of enzyme HDAC8, it is classified as a zinc-dependent class I HDAC, containing 377 amino acids (Buggy *et al*, 2000; Hu *et al*, 2000; Van den Wyngaert, 2000). Of note, HDAC8 is a zinc-dependant enzyme. Noticeably, about a decade ago, the role of zinc in gene expression has begun to attract interests and this field has recently gained wide attention. The mere existence of zinc in a wide range of proteins was widely known to have important impacts on the metabolism of most organisms (Roohani *et al.*, 2013). Zinc metalloenzymes are taken into consideration as the significant targets for such diseases as cancer, heart disease, bacterial infection, and Alzheimer's disease (Santos-Martins *et al.*, 2014). More importantly, hydroxamic acid is the most commonly used ZBG (zinc binding group) for its strong binding affinity with the zinc ion (Zhang *et al.*, 2018). By the analysis of the crystal structure of the inhibitor – receptor complex, it was elucidated that hydroxamic acid binds to the zinc ion in a chelating manner which is considered as a guarantee of inhibitor activity (Zhang *et al.*, 2018).

Despite efforts on studying about hydroxamic acid derivatives, selective inhibitors of HDAC8 with properties in advanced preclinical/clinical models are still scarce (Charkrabarti *et al.*, 2015). The first HDACs inhibitor received the market approval from the FDA in 2006 was SAHA (Fig. 1A), a pan - HDAC inhibitors, hitting different isotypes all at once (Grant *et al.*, 2007). Nevertheless, recent reports have indicated that side effects related to SAHA are bone marrow depression, diarrhea, weight loss, and taste disturbance (Chang *et al*., 2004; Montgomery *et al*., 2008; Haberland *et al*., 2009), showing that the use of SAHA still remains problematic. These consequences are due to the inhibition of broad-spectrum HDAC members, not only the isotypes that cause cancers (Oehme *et al.*, 2009). Hence, to minimize these clinical side effects, searching for an HDAC8 inhibitor is in urgent need.

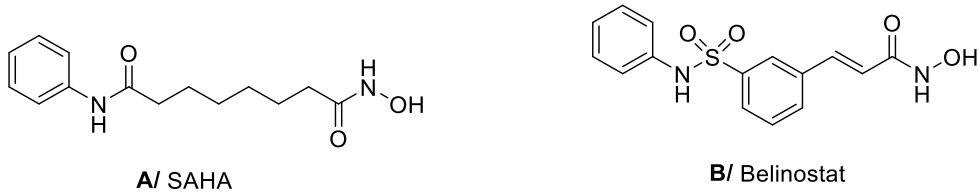

A/ SAHA **B/** Belinostat

Fig. 1: The structure of SAHA and Belinostat

According to this unique structure of HDAC8, belinostat (Fig. 1B), another member of hydroxamic acid class, has appeared to be a potential candidate with two characteristics to successfully inhibit the enzyme and limit side effects compared to other HDAC inhibitors. To be more specific, belinostat possesses features of a HDAC8 selective inhibitor. Firstly, it belongs to hydroxamic acid group, which was characterized by the ability to form chelate with the zinc ion at the foot pocket. Secondly, it is a short meta-substituted cinnamic acid linker, which is expected to fit well to the active site of HDAC8 (Krennhrubec *et al*., 2007). Additionally, belinostat passed all of the pre-clinical and clinical trials with out of expected results and has received the market approval from FDA in 2014 for the

treatment of patients with relapsed and refractory peripheral T-cell lympomas (PTCL) (Barneda-Zahonero and Parra, 2014). This proves that belinostat does not only stand out for the well-fitted structure with the binding site of HDAC8 but also the safety and large scale it guarantees compared to other HDAC8 selective inhibitors still produced under lab scale and experimented in vitro tests. Therefore, if belinostat demonstates good capabilities to inhibit HDAC8, it will be expected to expand the treatment for other HDAC8-related diseases. To testify the postulation, by means of docking simulation using Autodock forcefield, an attempt was made to analyze the interactions between HDAC8 and belinostat to evaluate the inhibition level of belinostat. Potential problems associated with zinc ion were investigated by the aid of Autodock4Zn.

2 MATERIALS AND METHOD

2.1 Ligand Preparation

All calculations were performed with the aids of the Gaussian 09 program. The geometries were fully optimized, making use of the functional B3LYP in conjunction with the 6-311++G(d,p) basis set for carbon and hydrogen atoms for belinostat.

2.2 Protein Preparation

HDAC8: The crystal structure of HDAC8 in complex with a hydroxamic acid inhibitor (PDB code:1t67) was retrieved from the Protein Data Bank (PDB; https://www.rcsb.org/structure/1t67) (Fig. 2A). All water molecules and small molecules were deleted except the Zn^{2+} ion coordinating with hydroxamic acid, which were kept for the docking step as shown in (Fig. 2B).

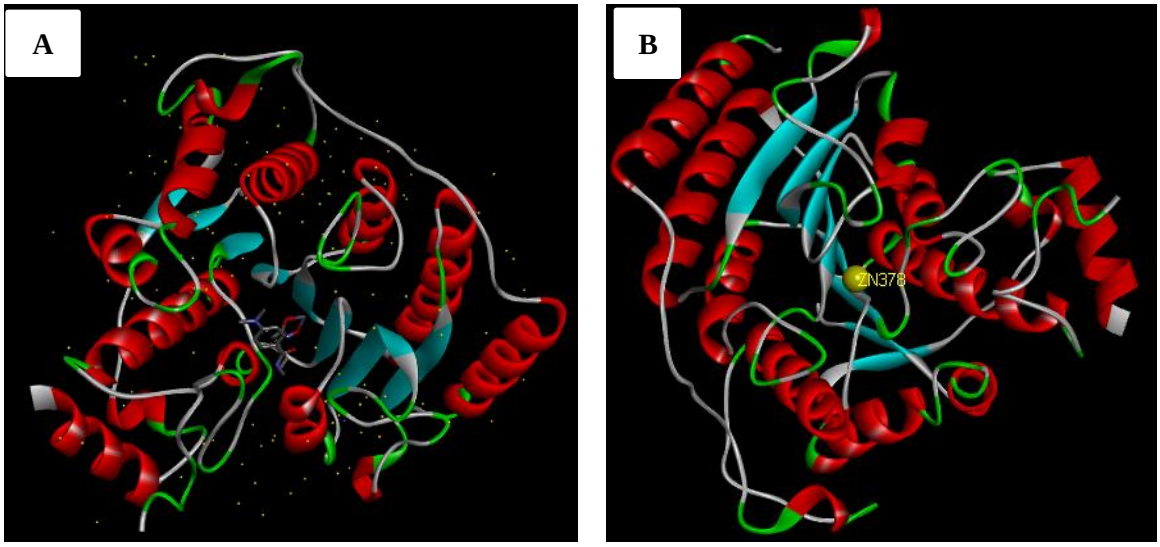

Fig. 2: A/ Crystal structure of Human HDAC8 in complex with MS-344

B/ Crystal structure prepared for docking

2.3 Docking

Autodock Tool version 4.2.6 was used in the docking studies including 3 steps:

1. Grid parameters: Autogrid was carried out to pre-calculate grid maps of interaction energies between the atoms of ligand and protein. The receptor grid preparation for the docking procedure was implemented by assigning the macromolecule as the center of the grid box and comprised 70 × 70 × 70 points with 1 Å spacing (Fig. 3A). Grid input file also included the AD4Zn.dat, which is a specific parameter file for zinc ion.

2. Autodock Vina program was run to find out 10 sites in which lowest energy estimations between ligand and receptor were given.

3. Autodock4 program was used for docking purposes with the binding site chosen among ten sites from the Vina step.

In this step, the ligand was redocked into the binding pocket obtained from the step 1 by using the Autodock program. Grid box parameters was set to cover all the residues around the binding pocket. More specifically, it was centered on the ligand and

comprise 126 × 126 × 126 points with 0.15 Å in spacing (Fig. 3B).

The Lamarckian Genetic Algorithm was used to explore the best conformational space for the ligand with 100 docking runs for each ligand. The maximum numbers of generation and evaluation were set at 27,000 and 50,000,000, respectively. Other parameters were set as default. After docking process completed, 100 conformations of the ligands in complex with the receptor were obtained and ranked based on binding energy (Thien, 2019).

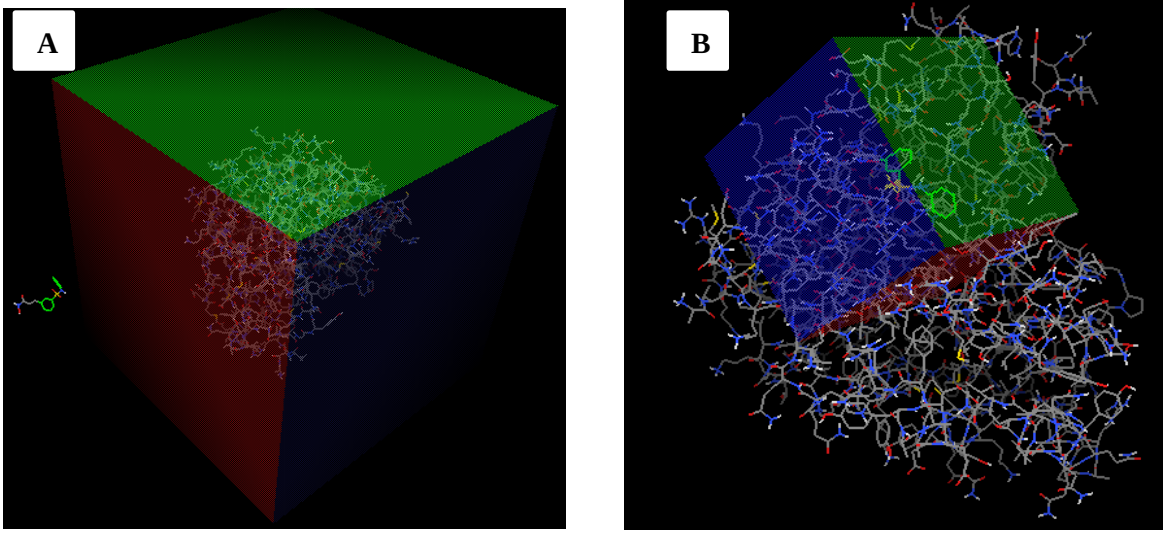

Fig. 3: A/ Grid box parameter set in docking calculations (70 × 70 × 70)

B/ Grid box parameter set for redocking step (2nd step) (126 × 126 × 126)

3 RESULTS AND DISCUSSION

3.1 Reinforcing the accuracy of the method by comparing the active site

In order to assess the accuracy of the Autodock4.2.6 program using for docking belinostat (Fig. 4B) into HDAC8, the crystal structure of MS-344 (a SAHA-like compound) (Fig. 4A) and HDAC8 was retrieved from the Protein Data Bank (PDB code: 1t67) to compare the active site and binding modes between the ligand and the protein.

A typical structure of a HDAC inhibitor consists of three main domains: the surface recognition domain of the inhibitors interacting with the external surface of the enzyme, the hydroxamic acid group acting as a metal binding domain at the bottom of the pocket and a linker to connect these two domains. (Finnin *et al.*, 1999).

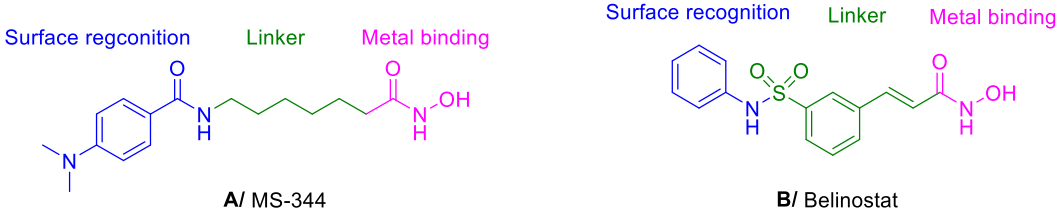

A/ MS-344 **B/** Belinostat

Fig. 4: Chemical structures of MS-344 (a SAHA-like compound) and Belinostat

When it comes to the mode of binding between a HDAC inhibitor and its corresponding enzyme, the coordination state of zinc ion is the precondition for the inhibitors to exert their inhibitions. Hydrogen bonds and hydrophobic interactions were also examined to analyze its stability. Firstly, there are similarities between the two pockets presented here (Fig. 5A and 5B), the tunnel is filled by the aliphatic chain (MS-344) and the phenylene chain (belinostat) of the inhibitor. Secondly, the walls of the tunnel are formed by Phe152, Phe208, His180, Gly151 and Tyr306 (Fig. 5F). Finally, the coordination state of the zinc ion (yellow color) (Fig. 5B and 5D) was also investigated because zinc ion is very important for the catalytic activities of HDACs. The catalytic machinery is placed at the

end of the hydrophobic tunnel. The centerpiece of this region is a zinc-ion Zn378 that is binded to carboxylate oxygens of the ligand. Although Belinostat is not capable of forming the zinc chelate, it still can make contact to the ligand by covalent bond (Fig 5A, 5C, 5E). Based on the typical characteristics of the binding site between MS-344 and HDAC8 listed above, it can be concluded that belinostat is able to enter the active site of HDAC8.

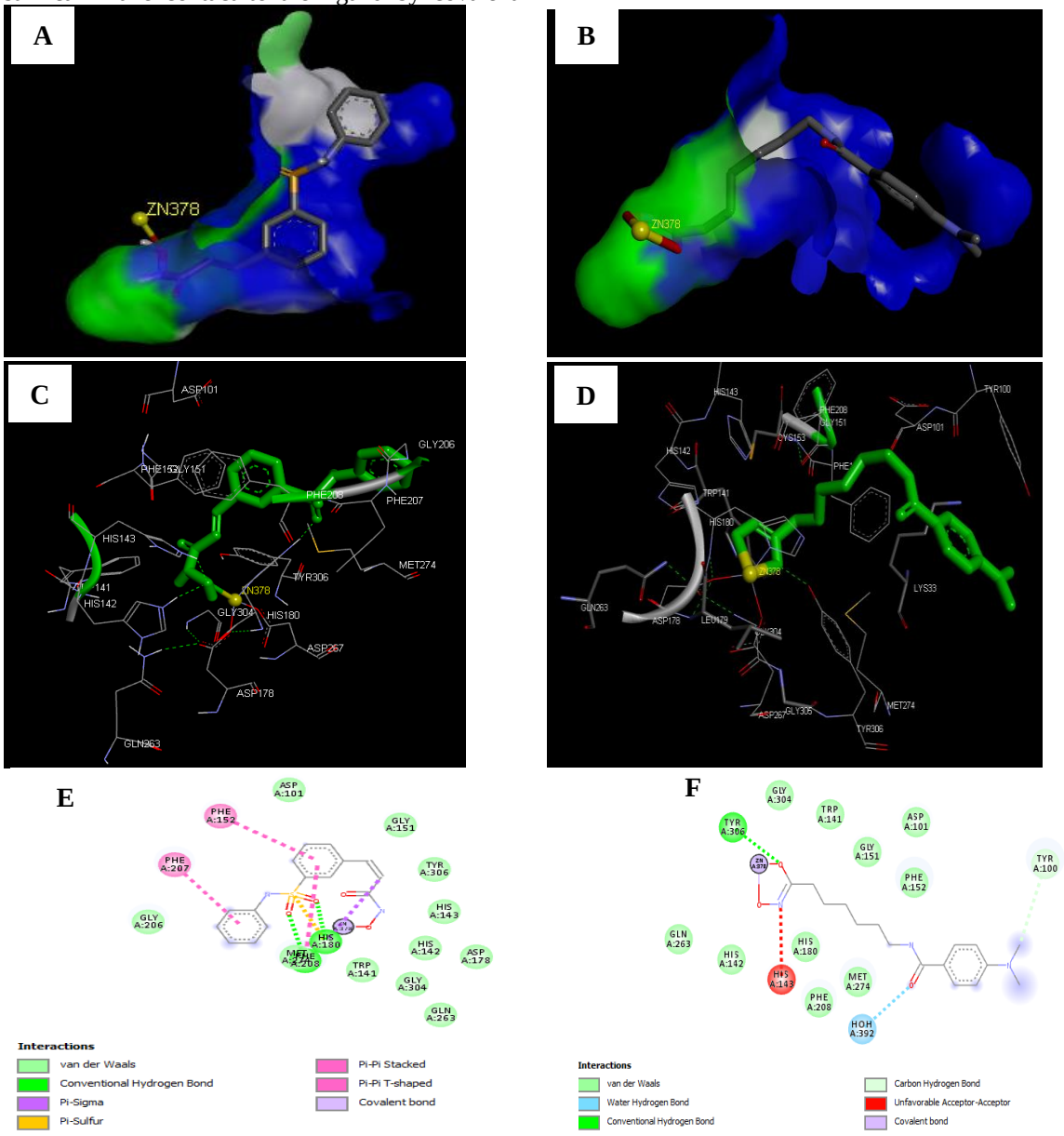

Fig. 5: Molecular docking results of Belinostat and MS-344

A/ The active site of HDAC8 and Belinostat (Zn: yellow color)

B/ The active site of HDAC8 and MS-344 (Zn: yellow color)

C/ 3D binding model of Belinostat into the HDAC8 (Zn: yellow color)

D/ 3D binding model of MS-344 in the active site of HDAC8 (Zn: yellow color) (https://www.rcsb.org/structure/1t67)

E/ 2D binding model of Belinostat in the active site of HDAC8 (Zn: grey color)

F/ 2D binding model of MS-344 into the HDAC8 (Zn: grey color)

3.2 Investigation of the binding mode between Belinostat and HDAC8

Since the structure of belinostat comprises three parts: surface regconition group or capping group (CP), linker and zinc binding group (ZBG) (Fig. 6A). The investigation of the binding in each part was carried out separately. Firstly, regarding the coordination state of the zinc ion, it should be noticed that the ZBG bond is expected to be stronger than other interactions as the ZBG is polarized by the zinc ion. Therefore, this interaction makes up most of the ligand binding energy. In the current docking result, regardless of failing to form chelate complex between the hydroxamic acid and Zn378, it was able to have contact with belinostat by a covalent bond.

Apart from ZBG, the linker also accounts for predominant interactions. It is embedded in a lipophilic channel whose walls consist of Phe152, Phe208, His180, Gly151 and Tyr306 (Fig. 5C and 5E). Similar to other HDAC inhibitors with aromatic short linkers, the aromatic rings of this series of HDACIs are also very important for their inhibitory activities. The pi-pi stacking establishment between the center aromatic group of belinostat and Phe152/Phe208 helps to stabilize the linker in the pocket. Another bond which is the pi-sigma interaction between the vinyl group of belinostat and His180 also contributes to the stabilization of the complex (Fig. 5E). Additionally, the sulfonamide group presents significant interactions. To be more precise, not only did the two thionyls of sulfonamide group form hydrogen interaction (green binding) with Phe208 and His180 but the sulfur atom also bonded with HDAC8 residue His180 by pi-sulfur interaction (orange binding) (Fig. 5C and 5E).

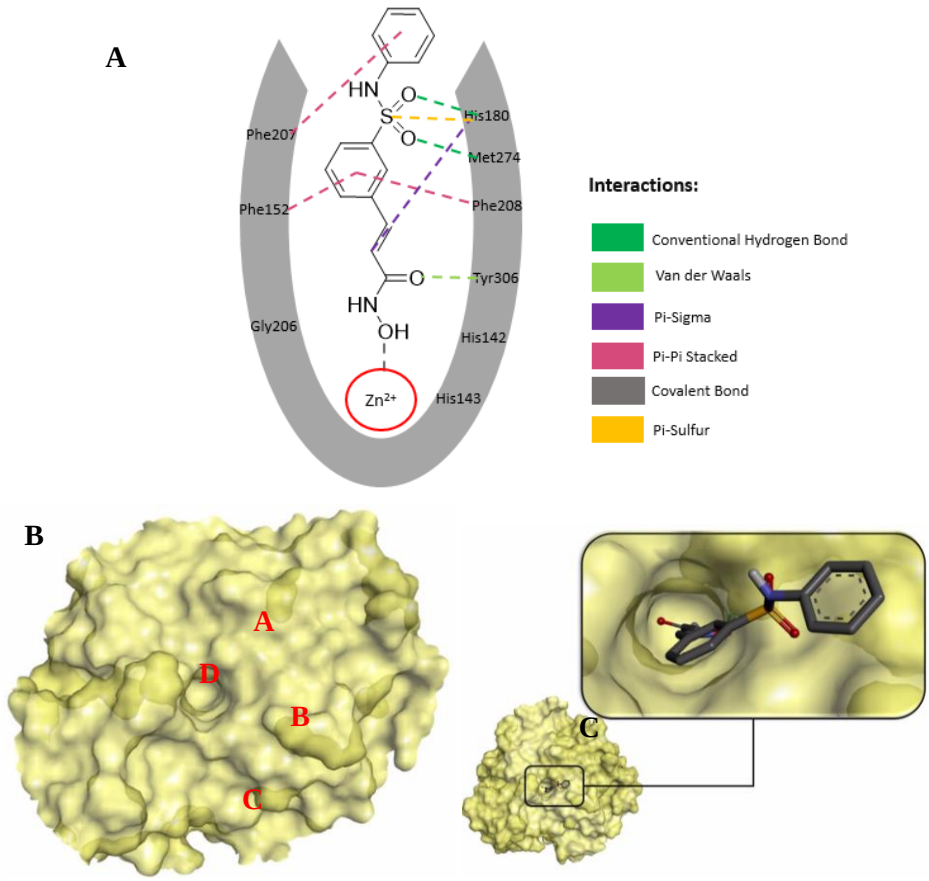

Fig. 6: Binding interaction between HDAC8 and belinostat in the active site pocket

A/ The simulation of the binding site between HDAC8 and belinostat

B/ The surface of the active site of HDAC8 divided into four regions

C/ 3D binding model illustrating the interaction between HDAC8 and belinostat

Directly connecting with the CP is the surface of the active site, which is normally divided into four areas: the first one determined by Lys33 and Met274 (A), the second by Met274 and Phe207 (B), the third by Gly206 and Asp101 (C), and the smallest by Tyr100 and Lys33 (D) (Fig. 6B and 6C) (Ortore *et al.*, 2009). Belinostat only shows connection with the B region where the aromatic group connects the His207 residue through a pi-pi stacking interaction (pink binding). Owing to hydrophobic contacts and hydrogen bonds, belinostat elucidates itself to be a potent selective-HDAC8 inhibitor, with a low binding energy estimation and inhibition level (-8.97 kcal/mol and 265.3 nM respectively). The binding energy estimation is approximately equal to a previous report, at -8.68 kcal/mol, proving the accuracy and reliability of the results (Uba and Yelekci, 2017).

4 CONCLUSIONS

With the support of Autodock Tool including Autodock4 and Autodock4Zn, the interaction between Belinostat and the active site of a novel target for cancer treatment - HDAC8 enzyme was ultimately explored. The results show hydrophobic interactions established by aromatic groups with Phe152, Phe207 and Phe208, hydrogen bonds arising from the sulfonamide group and especially the binding between zinc ion and the hydroxamic acid group. All of which are necessary for stabilizing the ligand - protein complex and hence bettering the inhibition of HDAC8 activity of belinostat. Overall, with this result, belinostat proves itself to be an effectively selective HDAC8 inhibitor, contributing to further applications on the cancer treatment of HDAC-induced diseases.

ACKNOWLEDGEMENT

Our research team is very grateful for the financial support from Can Tho University for this study (Code: TSV2019-48).

REFERENCES

Balasubramanian, S., Ramos, J., Luo, W., Sirisawad, M., Verner, E., & Buggy, J. J., 2008. A novel histone deacetylase 8 (HDAC8)-specifc inhibitor PCI-34051 induces apoptosis in T-cell lymphomas. Leukemia. 22(5): 1026–1034.

Barneda-Zahonero, B., & Parra, M., 2012. Histone deacetylases and cancer. Molecular Oncology, 6(6): 579-589.

Buggy, J. J., Sideris, M. L., Mak, P., Lorimer, D. D., Mcintosh, B., & Clark, J. M., 2000. Cloning and characterization of a novel human histone deacetylase, HDAC8. Biochemical Journal, 350(1): 199-205.

Chakrabarti, Ina Oehme, Olaf Witt and *et al*., 2015. HDAC8: a multifaceted target for therapeutic interventions. Trends in Pharmacological Sciences. 36: 481-492.

Chakrabarti, A., Melesina, J., Kolbinger, F. R., *et al*., 2016. Targeting histone deacetylase 8 as a therapeutic approach to cancer and neurodegenerative diseases. Future Medicinal Chemistry. 8(13): 1609-1634.

Chang, S., McKinsey, T. A., Zhang, C. L., Richardson, J. A., Hill, J. A., & Olson, E. N., , 2014. Histone Deacetylases 5 and 9 Govern Responsiveness of the Heart to a Subset of Stress Signals and Play Redundant Roles in Heart Development. Mol. Cell. Bio. 24: 8467–8476.

Ruijter, A. J. D., Gennip, A. H. V., Caron, H. N., Kemp, S., & Kuilenburg, A. B. V., 2003. Histone deacetylases (HDACs): characterization of the classical HDAC family. Biochemical Journal, 370(3): 737-749.

Falkenberg, K. J., & Johnstone, R. W., 2014. Histone deacetylases and their inhibitors in cancer, neurological diseases and immune disorders. Nature Reviews Drug Discovery, 13(9): 673.

Finnin, M.S.; Donigian, J.R.; Cohen, A.; Richon, V.M.; Rifkind, R.A.; Marks, P.A.; Breslow, R.; Pavletich, N.P, 1999. Structures of a histone deacetylase homologue bound to the tsa and saha inhibitors. Nature, 401: 188–193.

Grant, S., Easley, C., & Kirkpatrick, P., 2007. Vorinostat.

Haberland M, M. R. O. E., 2009. The many roles of histone deacetylases in development and physiology: implications for disease and therapy. Nat Rev Genet. 10: 32-42.

Hu, E., Chen, Z., Fredrickson, T., et al., 2000. Cloning and characterization of a novel human class I histone deacetylase that functions as a transcription repressor. Journal of Biological Chemistry, 275(20): 15254-15264.

Huang, D., Li, X., & Xiu, Z., 2012. Molecular modeling of the interactions between histone deacetylase 8 and inhibitors. Journal of Theoretical and Computational Chemistry. 11: 907-924.

Kelly WK, O. O., K. L., C. J. *et al*., 2005. Phase I study of an oral histone deacetylase inhibitor, suberoylanilide hydroxamic acid, in patients with advanced cancer. J Clin Oncol. 23: 3923-3931.

KrennHrubec, K., Marshall, B. L., Hedglin, M., Verdin, E., & Ulrich, S. M., 2007. Design and evaluation of 'linkerless' hydroxamic acids as selective HDAC8 inhibitors. Bioorg. Med. Chem. Lett. 17(10): 2874–2878.

Oehme I, Deubzer HE, Wegener D *et al*., 2009. Histone deacetylase 8 in neuroblastoma tumorigenesis. Clin. Cancer Res. 15(1): 91–99.

Olson DE, Wagner FF, Kaya T et al., 2013. Discovery of the first histone deacetylase 6/8 dual inhibitors. J. Med. Chem. 56(11): 4816–4820.

Ortore, G., Colo, F. D., & Martinelli, A., 2009. Docking of hydroxamic acids into HDAC1 and HDAC8: a rationalization of activity trends and selectivities. Journal of Chemical Information and Modeling, 49(12): 2774-2785.

Ortore, G., Colo, F. D., & Martinelli, A., 2009. Docking of hydroxamic acids into HDAC1 and HDAC8: a rationalization of activity trends and selectivities. Journal of Chemical Information and Modeling, 49(12): 2774-2785.

Micelli, C., Rastelli, G., 2015. Histone deacetylases: structural determinants of inhibitor selectivity. Drug Discov. Today 20(6): 718–735.

Montgomery, R.L., Potthoff, M.J., Haberland, M., et al., 2008. Maintenance of Cardiac Energy Metabolism by Histone Deacetylase 3 in Mice. J. Clin. Invest. 118: 3588–3597.

Mottamal, M., Zheng, S., Huang, T. L., & Wang, G., 2015. Histone deacetylase inhibitors in clinical studies as templates for new anticancer agents. Molecules, 20(3): 3898-3941.

Morris, 2007. AutoDock. [Online]. Available at: http://autodock.scripps.edu/wiki/AutoGrid

Saha and Pahan, 2006. HDACs in neurodegeneration: a tale of disconcerted acetylation homestasis. Cell Death & Differentiation. 13: 539-550.

Somoza, J. R., Skene, R. J., Katz, B. A. *et al*., 2004. Structural snapshots of human HDAC8 provide insights into the class I histone deacetylases. Structure. 12: 1325-1334.

Parbin, S., Kar, S., Shilpi, A., Sengupta *et al*., 2014. Histone deacetylases: a saga of pertubed acetylation homeostasis in cancer. Journal of Histochemistry & Cytochemistry. 62: 11-33.

Santos-Martins, D., Forli, S., Ramos *et al*., 2014. AutoDock4Zn: An improved AutoDock forcefield for small-molecule docking to zinc metalloproteins. Journal of Chemical Information and Modeling. 54: 2371-2379.

Roohani, N., Hurrell, R., Kelishadi, R., & Schulin, R., 2013. Zinc and its importance for human health: An integrative review. Journal of Research in Medical Sciences: The Official Journal of Isfahan University of Medical Sciences, 18(2): 144.

Thien, H. D., 2019. Molecular docking studies of synthesized benzimidazole derivatives as Hepatitis C virus NS5B inhibitors. Master Thesis. Can Tho University. Can Tho City

Uba, A. I., & Yelekci, K., 2017. Exploration of the binding pocket of histone deacetylases: the design of potent and isoform-selective inhibitors. Turkish Journal of Biology, *41*(6): 901-918.

Van den Wyngaert, I., de Vries, W., Kremer, A., and *et al*., 2000. Cloning and characterization of human histone deacetylase 8. FEBS letters, 478(1-2): 77-83.

Walkinshaw, D. R., & Yang, X. J., 2008. Histone deacetylase inhibitors as novel anticancer therapeutics. Current Oncology, 15(5): 237.

Zhang, L., Zhang, J., Jiang, Q., *et al*., 2018. Zinc binding groups for histone deacetylase inhibitors. Journal of enzyme inhibition and medicinal chemistry, 33(1): 714-721.